Two-Parameter Study on the Jet Regurgitant Mode of Resonant Tube

*Se-Myong Chang, **Soogab Lee

Abstract

A conceptual simplified model of Hartmann-Sprenger tube is suggested and investigated to decouple the regurgitant mode in the present paper. In spite of high nonlinearity, the acoustic behavior of this resonant tube system is dependent on wavelength and depth of the tube. The effect of forcing frequency and tube geometry on jet regurgitant mode are studied and discussed. With a conventional axisymmetric Euler code, sensitive acoustic problems are solved and validated by comparison with analytic theories.

Classified Field Number: 10.7 Aero-acoustics

I. Introduction

Hartmann-Spenger tube with one end open and the other closed, installed on the aligned central axis of a supersonic under-expanded jet, undergoes a violent vibration with the compression of tube flow by the impinging jet [1]. This resonant tube is being nominated to the ultrasonic drying and fog dissipation as well as the ignition device of a rocket engine [2]. Since the phenomena was first reported by Hartmann [3], the research of resonant pulsatile jet noise has been matured in gas dynamics and aero-acoustics societies [4-6]. According to a reference literature [2], the resonant noise is classified by three modes: 1) jet instability mode, 2) jet screech mode, and 3) jet regurgitant mode. The first mode is due to the Kelvin-Helmholtz instability producing small toroidal vortexlets on the slip stream while the second is the high-frequency mode originated from the interaction of Mach waves and jet boundary [7]. The third mode can be decoupled from two other modes since it depends primarily on tube geometry.

A new conceptual model is introduced in this paper to focus on the jet regurgitant mode. The arbitrary frequency (ν) is enforced in a subsonic flow ($\overline{M}$ = 0.5), and the tube is installed horizontally along the central axis. Axisymmetric Euler equations are solved to obtain the flow field data on Cartesian grid systems. Two parameters, Helmholtz number and aspect ratio of the tube are studied to analyze this resonant problem.

II. Methodology

2.1. Definition of the Present Problem

As shown in Fig. 1, the computational domain consists of three parts: 1) inside the tube, 2) outside the tube, and 3) buffer region. When the inlet flow is compressed by the tube wall, it is radiated outside producing a reverse expansive wave which will be reflected and again radiated with a compressive wave: see Fig. 2. This is the regurgitation mechanism of a resonant tube [1]. However, this cyclic motion will fade out to a steady state unless there is any source of vibrational energy. If the oscillating buffer region enforced a resonant vibration, it would continue the periodic motion. Our primary interest is the vibrational frequency of the resonant flow produced by the present model.
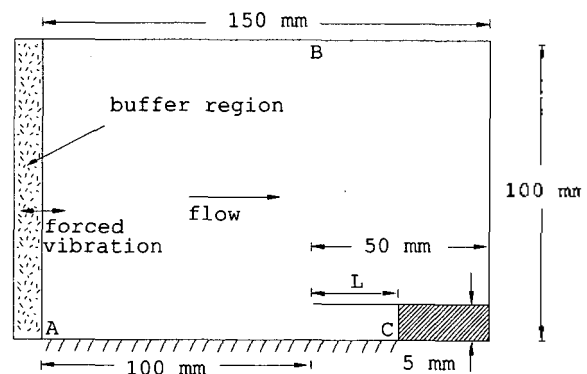

Figure 1. Definition of the present problem (half view).

* AANCL, Seoul National University
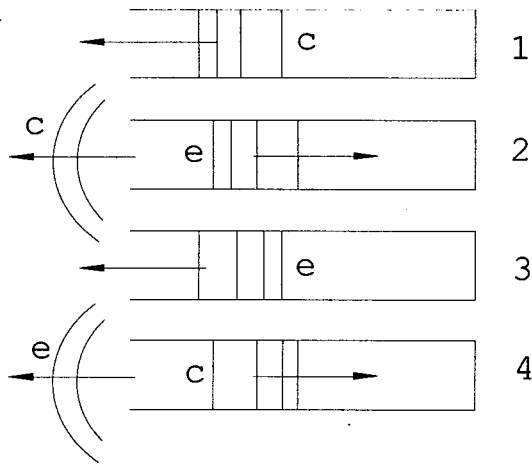** School of ME/AE, Seoul National University

Figure 2. Schematic for resonating cycle of jet regurgitant mode where c is compressive wave and e is expansive wave.

2.2. Parameters

Important variables in the present problem can be listed such as:

a_∞ : free-stream speed of sound

V_∞ : free-stream flow velocity

ν : flow oscillating frequency

l : distance between flow inlet and tube entrance

L : depth of tube

d : diameter of tube

Combining the above variables and applying Buckingham's pi theorem, four independent dimensionless numbers are obtained:

$$\Pi_1 = f_1(V_\infty, L, a_\infty) = \frac{V_\infty}{a_\infty} = M_\infty$$

$$\Pi_2 = f_2(V_\infty, L, \nu) = \frac{L\nu}{V_\infty}$$

$$\Pi_3 = f_3(V_\infty, L, l) = \frac{L}{l}$$

$$\Pi_4 = f_4(V_\infty, L, d) = \frac{d}{L}$$

The above are main parameters and their definition. An oscillatory flow field is enforced at the buffer region as mentioned in Section 2.1,

$$M(0, t) = \overline{M} + m\sin\omega t \qquad (1)$$

where

$$\omega = 2\pi\nu$$

and $\overline{M}$ and m are given. $d/l = \Pi_3\Pi_4$ is also fixed to 0.1 in Fig 1, and consequently the independent parameters in this study breaks down into the following two dimensionless variables:

$$K = \frac{\omega L}{a_\infty} = 2\pi\Pi_1\Pi_2 \qquad (2)$$

$$S = \frac{L}{d} = \Pi_4^{-1} \qquad (3)$$

where K is Helmholtz number and S is internal aspect ratio of the tube.

2.3. Numerical Strategy

Axisymmetric Euler equations for inviscid compressible flows are written down in the following tensor form [8]:

$$\frac{\partial U}{\partial t} + \frac{\partial F_j}{\partial x_j} + H = 0 : j = 1,2 \qquad (4)$$

where

$$U = \begin{pmatrix} \rho \\ \rho u_i \\ E \end{pmatrix}, \quad F_j = \begin{pmatrix} \rho u_j \\ \rho u_i u_j + p\delta_{ij} \\ u_j(E+p) \end{pmatrix},$$

$$H = \frac{1}{x_2} \begin{pmatrix} \rho u_2 \\ \rho u_i u_2 \\ u_2(E+p) \end{pmatrix} : i = 1,2 ,$$

and

$$E = \frac{p}{\gamma - 1} + \frac{1}{2}\rho u_j u_j$$

Eq. (4) is integrated with finite volume flux difference method based on Roe's approximate Riemann solver. The second-order accuracy for space and time is obtained by employing MUSCL algorithm [9]. This scheme is a kind of TVD high-resolution method using a slope limiter.

Flow tangency condition is applied at the wall and the symmetric axis of Fig. 1 is used for the computational domain. Along the free outer boundaries, non-reflecting boundary conditions are used, and inlet properties at the buffer region are modified using Eq. (1). If the inlet flow is choked, the mass flux is fixed. Additionally, the momentum is conserved and adiabatic process is assumed:

$$\rho u = \rho_\infty \overline{M} a_\infty \qquad (5)$$

$$p(1 + \gamma M^2) = p_\infty(1 + \gamma \overline{M}^2) \qquad (6)$$

$$\frac{p}{\rho}\{2 + (\gamma - 1)M^2\} = \frac{p_\infty}{\rho_\infty}\{2 + (\gamma - 1)\overline{M}^2\} \qquad (7)$$

Therefore, the forced boundary conditions at the left inlet in Fig. 1 are, from Eq. (5)-(7),

$$p(0, t) = p_\infty \frac{1 + \gamma \overline{M}^2}{1 + \gamma M^2(0, t)} \qquad (8)$$

$$\rho(0,t) = \rho_\infty \frac{2+(\gamma-1)M^2(0,t)}{1+\gamma M^2(0,t)} \cdot \frac{1+\gamma \overline{M}^2}{2+(\gamma-1)\overline{M}^2} \quad (9)$$

$$u(0,t) = \overline{M}a_\infty \frac{1+\gamma M^2(0,t)}{2+(\gamma-1)M^2(0,t)} \cdot \frac{2+(\gamma-1)\overline{M}^2}{1+\gamma \overline{M}^2} \quad (10)$$

2.4. Benchmark Validation

The Euler code is validated for a benchmark problem, acoustic wave propagation in a sonic pipe flow: see Fig. 3a. The entry Mach number, $M(0,t)$ is given in Eq. (1) by setting $\overline{M}$ = 1.0 to solve Eq. (4) with the code described in Section 2.3. From Eq. (1) and (8), the asymptotic series expansion for entry pressure becomes

$$p(0,t)=p_\infty\left\{1-\frac{2\gamma}{\gamma+1}\,m\sin\omega t+\frac{\gamma(3-\gamma)}{(\gamma+1)^2}\,m^2\sin^2\omega t- \ldots \ldots\right\}$$

If $m \ll 1$, the high-order terms are negligible:

$$p(0,t) = p_\infty\left\{1-\frac{2\gamma}{\gamma+1}\,m\sin\omega t\right\} \quad (11)$$

This perturbed signal is transmitted to downstream direction with $2a_\infty$ (speed of sound a_∞ plus mean flow velocity a_∞) and its angular frequency becomes 2ω by Doppler effect [10].

$$p(x,t) = p_\infty\left\{1-\frac{2\gamma}{\gamma+1}\,m\sin 2\omega(t-\frac{x}{2a_\infty})\right\} \quad (12)$$

Setting m = 0.1 and ν = 3.403 kHz, 1/10 cut-off frequency of the pipe, the pressure time history at the position x = 100 mm and its Fourier transformation are obtained in Fig. 3b-c.

From Eq. (12), the phase time is evaluated like:

$$\tau = t_{phase} - \frac{x}{2a_\infty} = 0 \text{ and } x = 0.1\,m \quad (13)$$

where τ is retarded time, and a_∞ = 340.3 m/s. The theoretical t_{phase} is therefore 14.69 ms, and 14.68 ms in case of Euler solution in Fig. 3b. The fundamental frequency in Fig. 3c is predicted to 2ν = 2 x 3.407 kHz, which has an error 0.11 %.
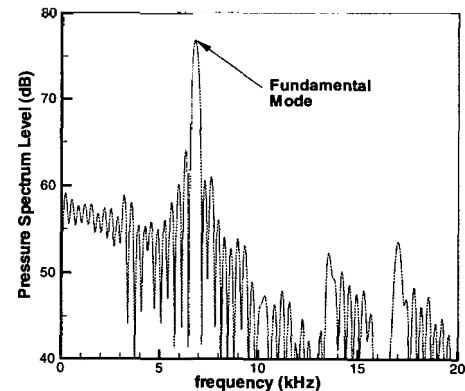
From this validation exercise, the dissipative error is shown to be very small at proper frequencies below the Nyquist value even for a delicate acoustic propagation problem. We expand this method directly to the nonlinear flow regime in the present problem.
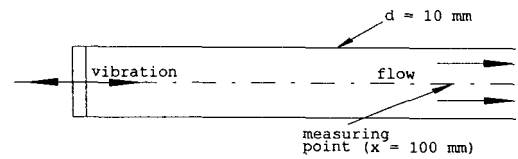
(a) Pipe flow with acoustic vibration
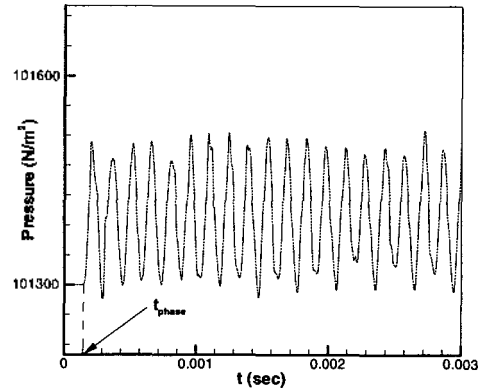
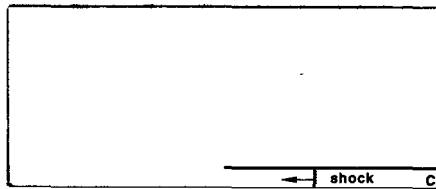(b) Pressure history at x = 100 mm

(c) FFT result of (b)

Figure 3a-c. Benchmark exercise: Acoustic propagation in sonic pipe flow.

## III. Distinguished Physics

3.1. Outline of Resonant Motion and Acoustic Propagation

Although there is no forced oscillation at the buffer region, the end wall of the tube generates a shock wave. Fig. 4a-d is the sequential pressure plots and streamlines of one cycle equivalent to Fig. 2, fixing $\overline{M}$ = 0.5, m = 0 (harmonic), and S = 5. In Fig. 4a, the shock propagates to left. When the shock is radiated to outer field in Fig. 4b, the expansive wave goes reversely to the right. In Fig. 4c, after the expansion wave is reflected from the end wall, it goes to the entrance of tube until a reverse compressive wave be generated: see
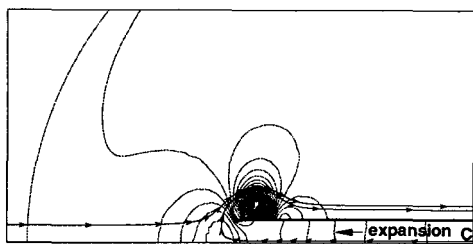
Fig. 4d. Fig. 4e is the pressure history at the point C, and Fig. 4f is its Fourier transform. The amplitude of regurgitant mode is being decayed to the steady state because no energy is added to this system.
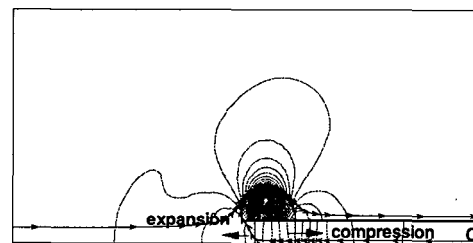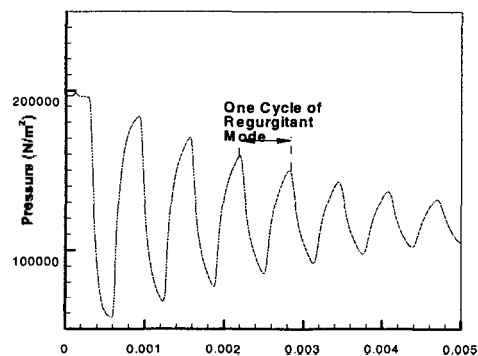

(a) t = 100 μs

(b) t = 200 μs

(c) t = 400 μs
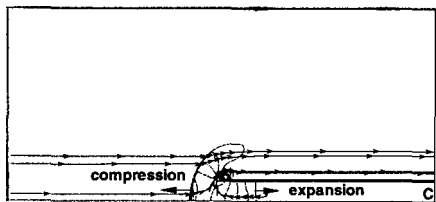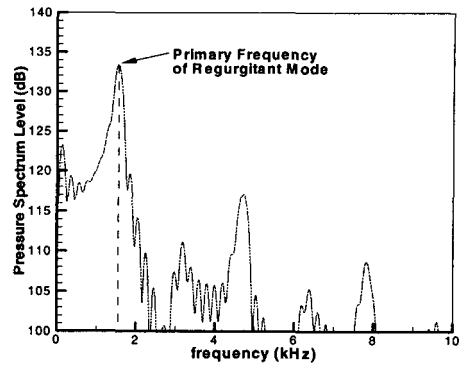

(d) t = 500 μs

(e) Pressure history at point C

Figure 4a-f. Regurgitant mode of a tube in the subsonic flow, $\overline{M}$ = 0.5.

However, the acoustic signals at the far field show a strange mode. The pressure histories and frequencies at the position A and B in Fig. 5a-d all serve a strong component (inside the dashed circle) other than regurgitant mode. This noise is steadily found except for the first resonant cycle, and suspected to be the effect of strong interaction of vortex and horizontal outer tube wall: see Fig. 4c-d.
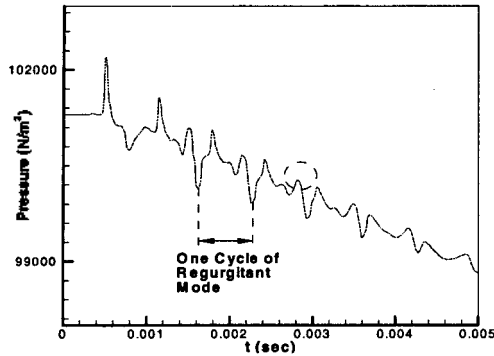
Fig. 4f indicates that the primary resonance frequency is ν_{res} = 1.554 kHz. If the one-dimensional theory is referred, the closed-end organ pipe best transmits acoustic energy at
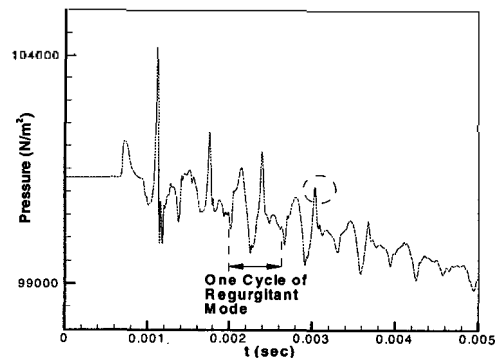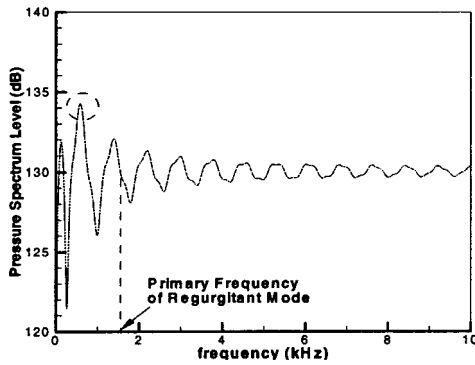

(a) Pressure history at point A
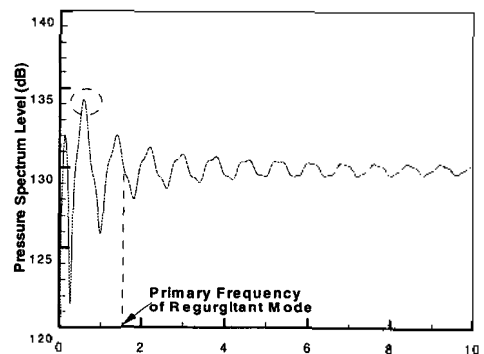
(b) FFT result of (a)

(c) Pressure history at point B

(d) FFT result of (c)

Figure 5a-d. Acoustic characteristics in the flow of Fig. 4a-f.

$$\nu_{res} = n\frac{a_\infty}{4L} \tag{14}$$

where n is an odd integer, and $n = 1$ is the primary resonance frequency [9]. The predicted primary value is $\nu_{res} = 1.702$ kHz (8.70 % error), and the discord with numerical result is due to nonlinearity originated from the fact that the streamline of incident flow is slightly deflected in front of the tube and the 'effective tube depth' is longer than its geometric depth: see Eq. (14) where the frequency is inversely proportional to the depth.

3.2. Parametric Study I : Forcing Frequency

Two cases are studied for different Helmholtz numbers: $K = 1$ ($\nu = 1.082$ kHz) and $K = 25$ ($\nu = 27.06$ kHz) fixing $\overline{M} = 0.5$, $m = 0.2$, and $S = 5$. Fig. 6a-c are pressure histories at the point A, B, and C marked in Fig. 1, and Fig. 6d shows the Fourier transform of Fig. 6c.

Comparing the reflected wave patterns at point B for the same forcing amplitude at point A, Fig. 6a, the high frequency wave is so evanescent or dissipative both numerically and physically that it showed much more decay: see Fig. 6b. The low frequency wave even can enhance the regurgitant mode in Fig. 6c, but its effect is valid for only first cycle. Moreover, the input frequency does not significantly change the natural mode shape: see Fig. 6d.
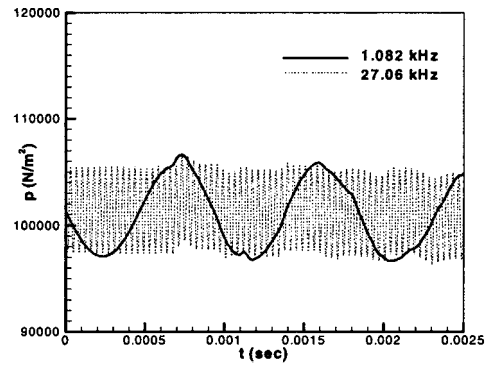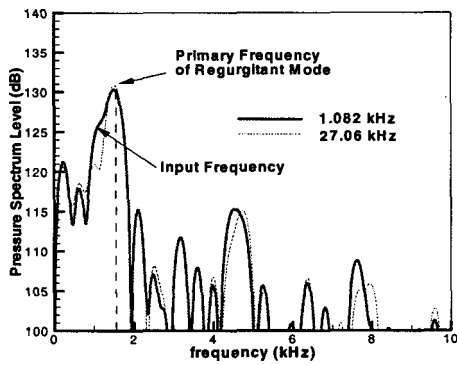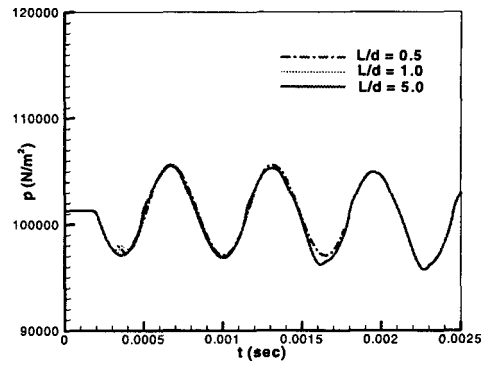

(a) Pressure history at point A
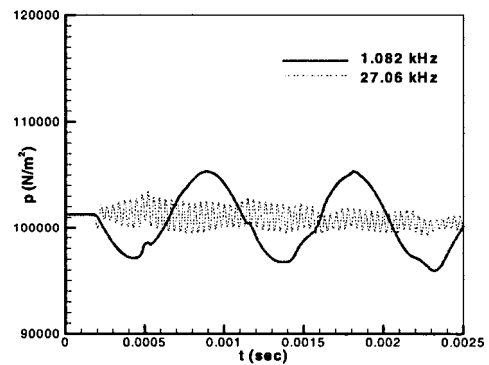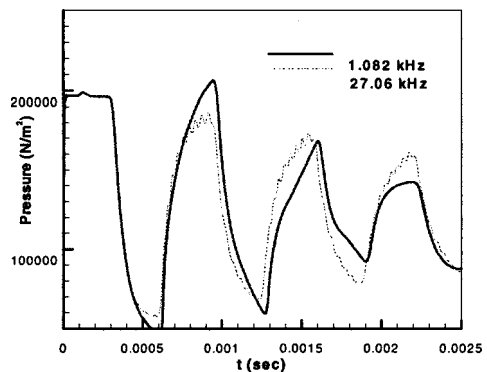
(b) Pressure history at point B

(c) Pressure history at point C
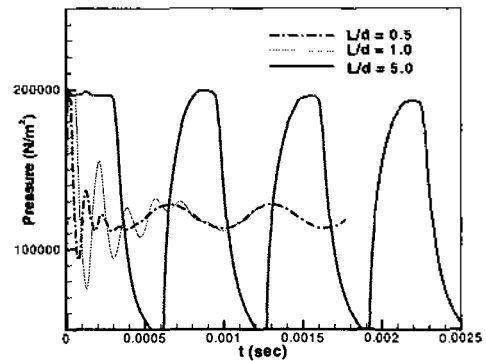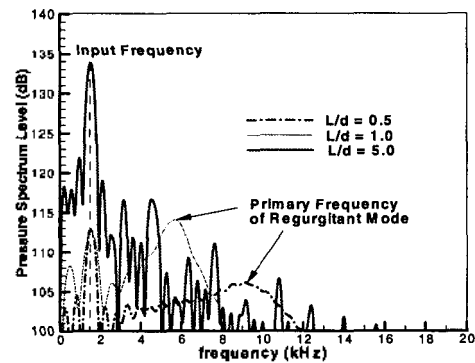
(d) FFT result of (c)

Figure 6a-d. Effect of frequencies.

3.3. Parametric Study II: Depth of Tube

Three cases are studied for different aspect ratios: S - 0.5, 1, and 5 fixing $\overline{M}$ - 0.5, m = 0.2, and ν = 1.554 kHz (primary resonance frequency of S = 5 case). Fig. 7a-c are pressure histories at the point A, B, and C marked in Fig. 1, and Fig. 7d shows Fourier transforms of Fig. 7c.

In Fig. 7a-b, except for some noises, the forcing acoustic wave is observed directly everywhere in the flow field. We can not easily discern the regurgitant mode itself in the far-field sound signals, Fig. 7b, for the first two cases. If the forcing frequency is not resonance one, the regurgitant motion is rapidly decayed but, for the third case of resonant frequency in Fig. 7c, remained periodic. After the resonant cycles are evaporated, the forcing frequency appears dominant in the full flow region: see Fig. 7d and also Fig. 7a-b. The regurgitant frequency obviously depends on its depth as shown in Fig. 7c. According to one-dimensional classical theory, Eq. (14), the regurgitant frequency should be inversely proportional to tube depth. In the present problem, the resonant frequency is 9.109 and 5.717 kHz for S = 0.5 and 1 cases respectively.
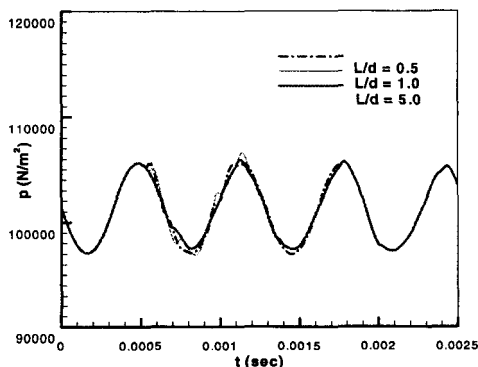

(a) Pressure history at point A

(b) Pressure history at point B

(c) Pressure history at point C

(d) FFT result of (c)

Figure 7a-d. Effect of tube depth.

IV. Concluding Remark

As mentioned in Section 2.2, the Hartmann-Sprenger tube has four independent parameters. Two of them, K and S, are investigated for the simplified model. Sinusoidal, but high-amplitude perturbations are enforced at the inlet for a subsonic flow. In Fig. 8a, the Mach disk in a sonic jet is vibrated, which enforces resonant energy to the system. The present model simplifies the shock only to oscillatory Mach number: see Fig. 8b.
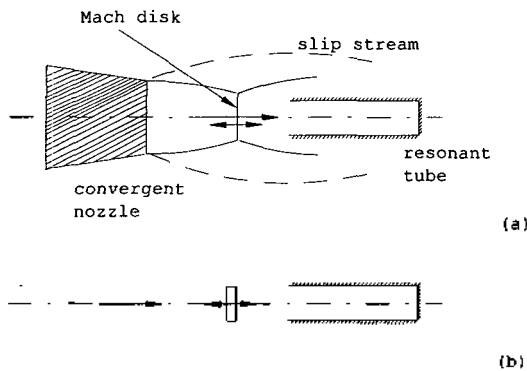
Figure 8a-b. Comparison of real physics and this model:
(a) Hartmann-Sprenger tube,
(b) the present problem.

As a result, the meaningful arguments are listed like the following:

1) In spite of the nonlinearity of phenomenon, the resonance frequency is a function of tube depth, and the wavelength is the most important parameter determining whether it will be evanescent or not.

2) The jet regurgitant mode is temporarily enhanced by the frequency similar to resonant value, but soon decays more rapidly. It is only remarkably amplified at the resonance frequency.

3) If the resonance frequency and forcing frequency coincide with each other, the regurgitant motion does not disappear, cycling long periodically. The regurgitation frequency depends on the depth of tube.

4) In the harmonic motion, the interaction of vortex and tube wall plays an important role of noise source. The deflection of streamlines before the entrance of tube increasing the effective depth induces a nonlinear effect on the resonance frequency.

5) The present scheme works well in this problem, but should be modified to higher-order one for more delicate studies on Computational Aero-Acoustics (CAA).

References

1. Yang H. D., Chang S. M. and Chang K. S., "Impingement of shock wave into a two-dimensional cavity," Journal of Korean Society for Aeronautics and Space Science, vol. 26, no. 8, pp. 11-19, 1998.

2. Sarohia V. and Back L. H., "Experimental investigation of flow and heating in a resonance tube," Journal of Fluid Mechanics, vol. 94, pp. 649-672, 1979.

3. Hartmann J., "On the production of acoustic waves by means of a air-jet of a velocity exceeding that sound," Philosophical Magazine, vol. 11, pp. 926-948, 1931.

4. Thompson P. A., "Jet-driven resonance tube," AIAA Journal, vol. 2, pp. 1230-1233, 1964.

5. Sobieraj G. B. and Szumowsk A. P., "Experimental investigations of an underexpanded jet from a convergent nozzle impinging on a cavity," Journal of Sound and Vibration, vol. 149, pp. 375-396, 1986.

6. Chang K. S., Kim K. H. and Iwamoto J., "A study on the Hartmann-Sprenger tube flow driven by a sonic jet," International Journal of Turbo and Jet Engines, vol. 13, pp. 173-182, 1996.

7. Ko S. M. and Chang K. S., "Resonant pulsatile flows of a Hartmann-Sprenger tube," Computational Fluid Dynamics Journal, vol. 6, pp. 439-452, 1998.

8. Sivier S., Loth E., Baum J. and Lohner R., "Vorticity produced by Shock Wave Diffraction," Shock Waves, vol. 2, pp. 31-41, 1992.

9. Chang S. M., "Unsteady shock wave-vortex interactions in the compressible shear layer," Ph.D. Thesis of KAIST, DAE965342, 2000.

10. Dowling A. P. and Ffowcs Williams J. E., Sound and Sources of Sound (John Wiley & Sons, New york, 1983), pp. 19-20, 63-74.

▲ Se-Myong Chang

Se-Myong Chang, Ph.D., is awarded his academic degree from Dept. Aerospace Engineering of KAIST in 2000, and now working as BK21 Post-doctoral Fellow at Seoul National University under the supervision of Prof. Soogab Lee. His research fields are aeroacoustics, shock-vortex interaction, and visualization of high-speed flow.

▲ Soogab Lee

Prof. Soogab Lee, Ph.D., finished his academic discipline at the Stanford University in 1992 with the award of Ballhaus Prize, and Research Scientist at NASA-Ames Research Center for 1992-1995. He has since served as a associate professor of School of Mechanical and Aerospace Engineering in Seoul National University. He is a member of Acoustical Society of Korea and the Korean Society for Noise and Vibration Engineering, actively working in aero-acoustics and noise control as a pioneer of this field in Korea.